# Supplementary Information for The Martian Boulder Automatic Recognition System (MBARS)

**Don R. Hood[1,2], S.F. Sholes[3,4], S. Karunatillake[5], C.I. Fassett[6], R.C. Ewing[2], J. Levy[7]**

[1]Department of Geosciences, Baylor University, Waco, Texas 76706, USA

[2]Department of Geology and Geophysics, Texas A&M University, College Station, Texas 77843, USA

[3]Department of Earth and Space Sciences, University of Washington, Seattle, Washington 98195, USA

[4]Jet Propulsion Laboratory, California Institute of Technology, Pasadena, California 91109, USA

[5]Geology and Geophysics Department, Louisiana State University, Baton Rouge, Louisiana 70803, USA

[6]NASA Marshall Space Flight Center, Huntsville, AL 35805, USA

[7]Department of Earth and Environmental Geosciences, Colgate University, Hamilton, New York 13346, USA

Corresponding author: Don Hood (Don_Hood@baylor.edu)

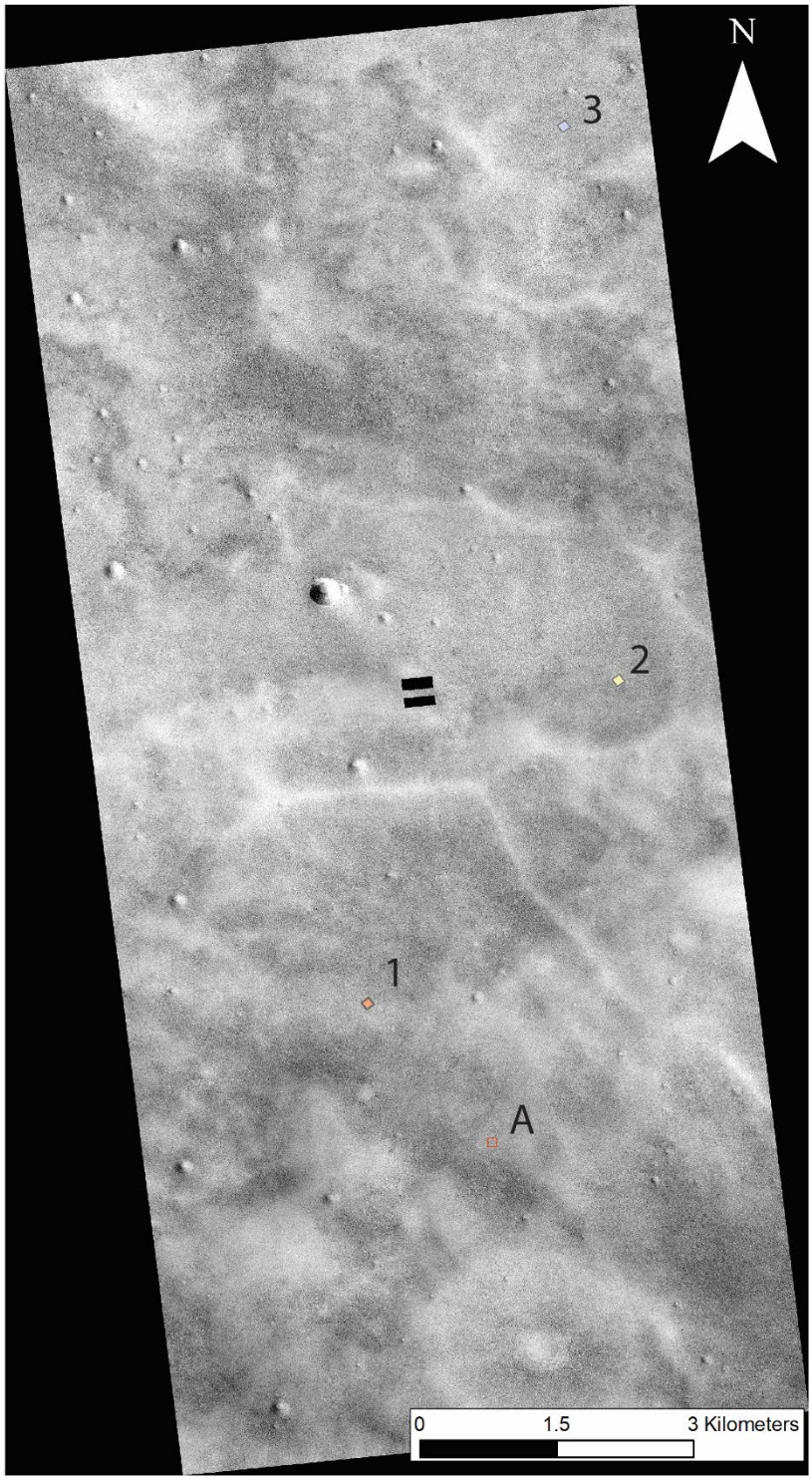


**Figure S1. PSP_007718_2350 with areas 1, 2, 3, and A labeled. Areas 1, 2, and 3 were measured in prior work (Sholes et al., 2017), and area A was measured for this work.**

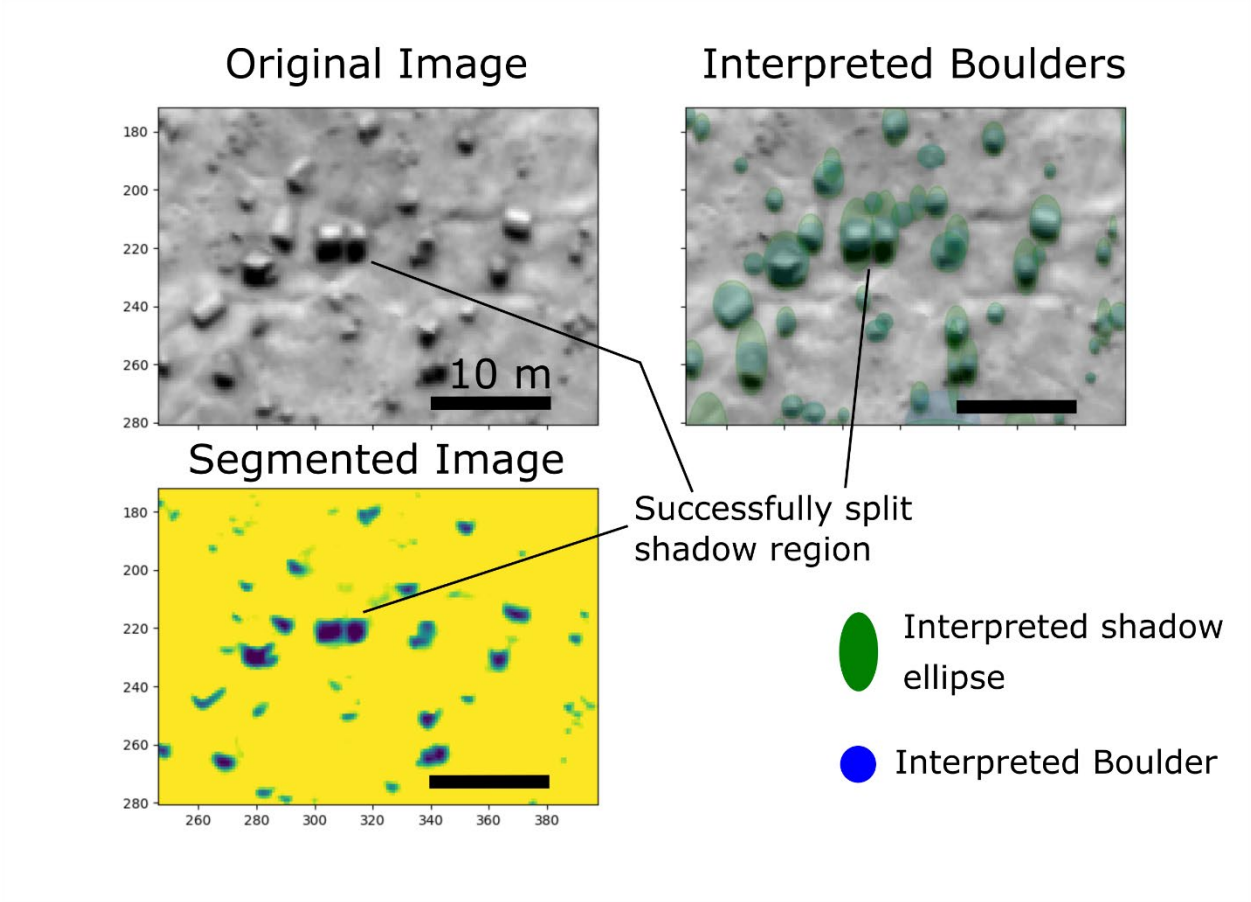


**Figure S2. A subset of HiRISE image TRA_000828_2495 with shadows shown with best-fit ellipses (green) and boulder models (blue disks). Ellipses are fit to the boundary of the shadows using Orthogonal Distance Regression. Shadows that lack ellipses were either removed due to small size or did not have good-fit ellipses. Two boulders with shadows that touch, forming a merged shadow region are successfully split by the algorithm.**

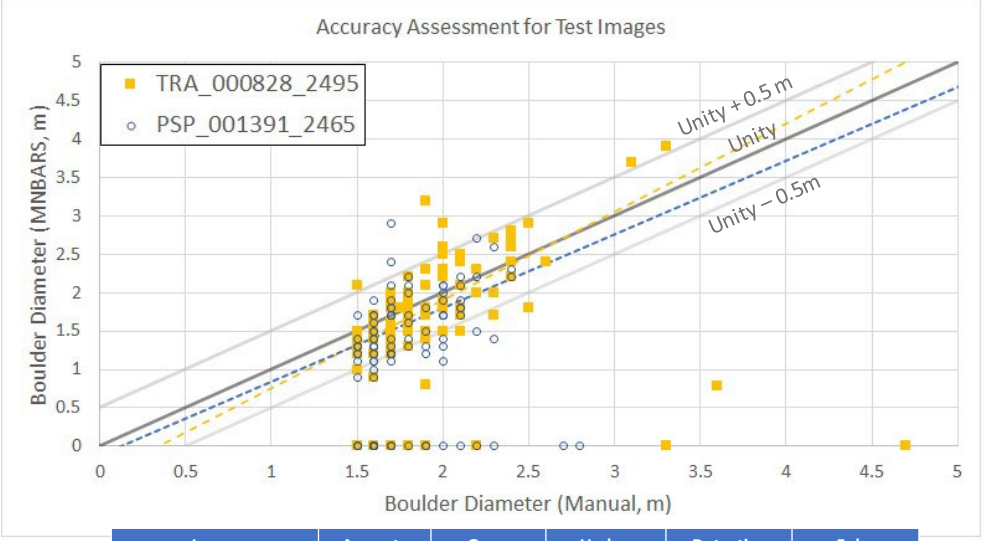


| Image | Accurate estimates | Over-estimates | Under-estimates | Detection Rate | False Negatives |
|---|---|---|---|---|---|
| TRA_000828_2495 | 76% | 6% | 8% | 90% | 10% |
| PSP_001391_2465 | 63% | 2% | 11% | 76% | 24% |

**Figure S3. Accuracy assessment for two test images using 100 boulders selected from intersections of a uniform grid. For each point on the grid, the nearest boulder with manually-determined diameter >1.5 m was marked and measured. Dashed lines represent linear regressions of the plotted data, excluding missed boulders and boulders >2.5 m. The trend for TRA_000828_2495 is >1, while the trend for PSP_001391_2465 is <1, but both are within one standard deviation of 1. Gray lines denote the 1:1 line (Unity) and ±0.5m, within which observations were considered accurate. Observations that fall on the x-axis were missed by MBARS and are noted as false negatives in the table.**

**Table S1. Collected final results table for images used in the testing of MBARS (excepting the images used for VL1, which were calibrated differently). The best-fit Rock Abundance (RA) and the $R^2$ of the fit are given for manual and MBARS results in each test area. Both the absolute RA error, and the RA error as a percentage of the manually-measured RA are given. Both errors vary widely, but at least one area within each image shows errors <0.1 RA, often the lower RA area of the two test areas.**

| Image | MBARS Boundary Parameter | Manual Area | RA | $R^2$ | MBARS RA | MBARS $R^2$ | RA Error | % RA Error |
|---|---|---|---|---|---|---|---|---|
| TRA_000828_2495_RED | 50 | A | 1.34 | 0.8 | 2.27 | 0.79 | 0.93 | 69.4 |
| | | B | 0.36 | 0.94 | 0.37 | 0.97 | 0.01 | 2.8 |
| PSP_001391_2465_RED | 40* | A | 0.42 | 0.97 | 0.55 | 0.86 | 0.13 | 31.5 |
| | | B | 0.19 | 0.99 | 0.16 | 0.96 | -0.02 | 10.9 |
| PSP_007718_2395_RED | 70 | 1** | 0.67 | 0.97 | 0.52 | 0.34 | -0.15 | 22.3 |
| | | 2** | 0.65 | 0.98 | 0.99 | 0.33 | 0.34 | 52.4 |

| | | | | | | | | |
|---|---|---|---|---|---|---|---|---|
| | | 3** | 1.13 | 0.99 | 1.23 | -1.21 | 0.10 | 8.5 |
| | | A | 0.80 | 0.99 | 0.92 | -0.66 | 0.12 | 14.6 |
| PSP_001501_2280_RED | 50 | A | 0.45 | 0.97 | 0.21 | 0.83 | -0.25 | 54.1 |
| | | B | 0.21 | 0.97 | 0.24 | 0.82 | 0.03 | 14.4 |
| PSP_001976_2280_RED | 60 | A | 0.45 | 0.97 | 0.23 | 0.80 | -0.23 | 50.0 |
| | | B | 0.21 | 0.97 | 0.28 | 0.94 | 0.07 | 32.6 |
| PSP_002055_2280_RED | 50 | A | 0.45 | 0.97 | 0.21 | 0.88 | -0.24 | 53.2 |
| | | B | 0.21 | 0.97 | 0.27 | 0.92 | 0.06 | 29.9 |

*: Note that these results were further filtered to better match the Manual analysis, See Section 3.3

**: These manual analyses come from prior work (Sholes et al., 2017)

**References:**

Sholes, S. F., Mushkin, A., & Catling, D. C. (2017). Boulder-Size Distributions as Indicators for Deposition Processes on Earth and Mars. In *GSA Annual Meeting*. Retrieved from http://dx.doi.org/10.1130/abs/2017AM-304073